Research Paper

Reversed Na$^+$/Ca^{2+} Exchange Contributes to Ca^{2+} Influx and Respiratory Burst in Microglia

Evan W. Newell[1,2]

Elise F. Stanley[1]

Lyanne C. Schlichter[1,*]

[1]Toronto Western Research Institute; University Health Network; and Department of Physiology; University of Toronto; Toronto, Ontario, Canada

[2]Current Address: Department of Microbiology and Immunology; Stanford University; Stanford, California, USA

*Correspondence to: Lyanne C. Schlichter; Toronto Western Research Institute; 399 Bathurst Street MC9-417; Toronto, Ontario, Canada; Tel.: 416.603.5970; Fax: 416.603.5745; Email: schlicht@uhnres.utoronto.ca

NOTE

A preliminary version of this work has been published as an abstract: EW Newell and LC Schlichter, Abstract 845.17 Society for Neuroscience Annual Meeting, Washington, Nov. 2005.

ABSTRACT

Phagocytosis and the ensuing NADPH-mediated respiratory burst are important aspects of microglial activation that require calcium ion (Ca^{2+}) influx. However, the specific Ca^{2+} entry pathway(s) that regulates this mechanism remains unclear, with the best candidates being surface membrane Ca^{2+}-permeable ion channels or Na$^+$/Ca^{2+} exchangers. In order to address this issue, we used quantitative real-time RT-PCR to assess mRNA expression of the Na$^+$/Ca^{2+} exchangers, *Slc8a1-3*/NCX1-3, before and after phagocytosis by rat microglia. All three Na$^+$/Ca^{2+} exchangers were expressed, with mRNA levels of NCX1 > NCX3 > NCX2, and were unaltered during the one hour phagocytosis period. We then carried out a biophysical characterization of Na$^+$/Ca^{2+} exchanger activity in these cells. To investigate conditions under which Na$^+$/Ca^{2+} exchange was functional, we used a combination of perforated patch-clamp analysis, fluorescence imaging of a Ca^{2+} indicator (Fura-2) and a Na$^+$ indicator (SBFI), and manipulations of membrane potential and intracellular and extracellular ions. Then, we used a pharmacological toolbox to compare the contribution of Na$^+$/Ca^{2+} exchange with candidate Ca^{2+}-permeable channels, to the NADPH-mediated respiratory burst that was triggered by phagocytosis. We find that inhibiting the reversed mode of the Na$^+$/Ca^{2+} exchanger with KB-R7943, dose dependently reduced the phagocytosis-stimulated respiratory burst; whereas, blockers of store-operated Ca^{2+} channels or L-type voltage-gated Ca^{2+} channels had no effect. These results provide evidence that Na$^+$/Ca^{2+} exchangers are potential therapeutic targets for reducing the bystander damage that often results from microglia activation in the damaged CNS.

ABBREVIATIONS

CR3, complement receptor 3; DPI, diphenylene iodonium; FBS, fetal bovine serum; HPRT1, hypoxanthine guanine phosphoribosyl transferase; IFNγ, interferon-gamma; IL1β, interleukin 1 beta; NADPH, nicotinamide adenine dinucleotide phosphate; NCX, Na$^+$/Ca^{2+} exchanger; NMDG$^+$, n-methyl d-glucamine; qRT-PCR, quantitative real-time reverse transcriptase polymerase chain reaction; SERCA, smooth endoplasmic reticulum calcium ATPase; SOC, store-operated Ca^{2+} channels; TNFα, tumor necrosis factor alpha

INTRODUCTION

As the resident immune cells of the CNS, microglia respond to damage or disease by undergoing a complex process of activation, in which dramatic changes in gene expression are accompanied by up-regulated cellular functions, including proliferation, phagocytosis, and production or release of reactive oxygen and nitrogen species, interleukins, cytokines and chemokines (recent reviews in refs. 1–12). Despite the presence in microglia of numerous receptor/ligand interactions that can elevate intracellular Ca^{2+} (Ca$^{2+}_i$), and the importance of Ca$^{2+}_i$ in many aspects of microglial activation (reviewed in refs. 13–17), there is a dearth of information about which influx pathway(s) regulate which microglial functions. While it is often assumed that such responses are mediated by store-operated Ca^{2+} permeable channels, the presence of functional Na$^+$/Ca^{2+} exchangers and members of the *Slc8a*/NCX family in microglia (reviewed in ref. 18) broadens the possibilities and deserves further consideration. In the normal mode, Na$^+$/Ca^{2+} exchangers cause Ca^{2+} efflux, but under certain conditions they can reverse to mediate Ca^{2+} entry. The objective of this study of rat microglia was to assess the conditions under which

reversed Na^+/Ca^{2+} exchange occurs and its potential contribution to the NADPH-dependent respiratory burst that accompanies phagocytosis. Reactive oxygen species liberated by the respiratory burst help degrade engulfed cellular debris but their extracellular release can also damage bystander cells, including neurons[19-22] (reviewed in ref. 23), especially when combined with nitric oxide to produce the membrane-damaging peroxynitrite.

We used real-time quantitative RT-PCR to determine which *Slc8a*/NCX genes are expressed and to compare their mRNA expression levels. Having observed that un-stimulated microglia can display depolarization-enhanced Ca^{2+} entry with several of the salient features of reversed-mode Na^+/Ca^{2+} exchange, we then characterized conditions under which such Ca^{2+} entry occurs and directly assessed its voltage dependence. While it was not technically feasible to analyze Ca^{2+} influx during the respiratory burst that accompanies phagocytosis, we used KB-R7943 to block activity of the reversed-mode Na^+/Ca^{2+} exchanger, in order to assess its role in this important aspect of microglial activation. Our results provide support for testing inhibitors of Na^+/Ca^{2+} exchangers in CNS pathologies in which damage by oxygen free radicals has been implicated.

MATERIALS AND METHODS

Microglia cultures. Microglia were isolated from brains of 2–3 day-old Wistar rats as we have previously described.[24-26] In brief, rat pups were sacrificed by cervical dislocation in accordance with guidelines from the Canadian Institutes of Health Research and the University Health Network. After carefully removing the meninges, whole brain tissue was mashed through a stainless steel sieve (100 mesh; Tissue Grinder Kit #CD-1; Sigma-Aldrich; Oakville, ON, Canada), and then pelleted, resuspended and seeded into flasks with Minimal Essential Medium (MEM) containing 5% fetal bovine serum (FBS), 5% horse serum, and 100 μM gentamycin (all from Invitrogen, Burlington, Canada). Two days later, cellular debris, non-adherent cells, and supernatant were removed and fresh medium was added to the flask. The mixed cultures were allowed to grow for 7–10 days and then shaken for 4 h on an orbital shaker at 8-10 Hz in a standard tissue culture incubator. The supernatant containing detached microglia was centrifuged and the cell pellet was resuspended for counting, and then plated at 3.5×10^4 cells per 15 mm diameter glass coverslip for electrophysiology. Before experiments, the plated microglia were cultured for 1–3 days in MEM with 100 μM gentamycin, and a reduced serum concentration (2% FBS) to maintain a more resting state. This procedure yielded 99–100% microglia, as judged by labeling with FITC-conjugated tomato lectin (see Fig. 2A) or isolectin B4 (both from Sigma-Aldrich); by immunofluorescence using the OX-42 monoclonal antibody (Serotec, Raleigh, NC), which recognizes complement receptor 3 (not shown); or by quantitative real-time RT-PCR.[25]

Quantitative real-time reverse transcriptase polymerase chain reaction (qRT-PCR). Transcript levels were monitored by real time quantitative RT-PCR (qRT-PCR),[27] as we recently described for microglia.[25,28-30] Gene-specific primers (Table 1) were designed using the 'Primer3Output' program (http://frodo.wi.mit.edu/cgi-bin/primer3/primer3_www.cgi). RNeasy mini kits (Qiagen, Mississauga, ON) were used to isolate RNA after degrading any contaminating DNA with DNaseI (0.1 U/ml, 15 min, 37°C; Amersham Biosciences, PQ). A two-step reaction was performed according to

Table 1 **Sequences of primers used for quantitative RT-PCR analysis**

Primer	Accession #	Sequence
HPRT1 (housekeeping)	NM_012583.2	F: CAGTACAGCCCCAAAATGGT
		R: CAAGGGCATATCCAACAACA
NCX1/*Slc8a1*	NM_019268	F: GATGAATGTGGGGAGGAGAA
		R: TTCTGTAGGTGGGACGAAGG
NCX2/*Slc8a2*	NM_078619	F: GTCACAGCCTCTTGGAGCAT
		R: AGAAGACCAGCGTGAGCAGT
NCX3/*Slc8a3*	NM_078620	F: CAAGAAGACCGCCAGCAT
		R: TCTCCCCCTTTCCTCACC
CR3	NM_012711	F: TGCTGAGACTGGAGGCAAC
		R: CTCCCCAGCATCCTTGTTT
$K_v1.3$	M30312	F: GCTCTCCCGCCATTCTAAG
		R: TCGTCTGCCTCAGCAAAGT

the manufacturer's instructions (Invitrogen); i.e., total RNA (1 μg) was reverse transcribed in 20 μl volume using 200 U of SuperScriptII RNase H-reverse transcriptase, with 0.5 mM dNTPs (Invitrogen) and 0.5 μM oligo dT (Sigma-Aldrich). Amplification was performed on an ABI PRISM 7700 Sequence Detection System (PE Biosystems, Foster City, CA) at 95°C for 10 min, followed by 40 cycles at 95°C for 15 s, 56°C for 15 s and 72°C for 30 s. 'No-template' and 'no-amplification' controls were included for each gene, and melt curves showed a single peak, confirming specific amplification.[27] The threshold cycle (C_T) for each gene was determined and normalized to that of the housekeeping gene, hypoxanthine guanine phosphoribosyl transferase (HPRT1). Since we studied the role of Ca^{2+}-entry pathways in the respiratory burst that resulted from phagocytosis of opsonized zymosan (see below), mRNA expression was examined with and without this stimulus.

Single-cell fluorescence imaging. Microglia on coverslips were mounted in a perfusion chamber (Model RC-25, Warner Instruments, Hamden, CT) and the tissue culture medium was replaced with standard bath solution containing (in mM): 135 NaCl, 5 KCl, 1 $MgCl_2$, 1 $CaCl_2$, 5 glucose, and 10 HEPES, adjusted to pH 7.4 (with NaOH) and to ~300 mOsm with sucrose. For ion-substitution experiments, NaCl was partly or completely replaced with KCl, NMDG-Cl or LiCl, as indicated. For the nominally Ca^{2+}-free solutions, $CaCl_2$ was omitted. EGTA was not added because we previously found that chelating all extracellular Ca^{2+} can promote spontaneous Ca^{2+} depletion,[31] which would compromise calibrating microglial Ca^{2+} levels from dye measurements. Images were acquired at room temperature using a Nikon Diaphot inverted microscope, Retiga-EX camera (Q-Imaging, Burnaby, BC, Canada), DG-4 arc lamp and excitation wavelength changer (Sutter Instruments, Novato, CA), and Northern Eclipse image acquisition software (Empix Imaging, Mississauga, ON, Canada).

To measure intracellular Ca^{2+}, microglia were loaded (~30 min, room temperature) with 3.5 μg/ml Fura-2-AM (Invitrogen, Burlington, ON, Canada) made in the indicated bath solution. Images were acquired at 340 and 380 nm excitation wavelengths, and ratios were obtained using a 505 nm dichroic mirror and 510 nm emission filter. In the representative figures, Fura-2 data are presented as the 340/380 nm ratio, and the summarized data in the text are presented as intracellular Ca^{2+} levels, calibrated (as previously

described[32]) using the values we determined for R_{min} (0.25 ± 0.002) and R_{max} (2.3 ± 0.097). Since we used 1 mM external Ca^{2+}, while 2 mM is often used in studies of microglia, we compared the effects of 1 vs 2 mM external Ca^{2+}. Resting intracellular Ca^{2+} was 70 ± 5 nM (56 cells) with 1 mM Ca^{2+} in the bath, 79 ± 5 nM after switching to 2 mM, and 85 ± 8 nM after returning to 1 mM (p > 0.2 for all comparisons). Hence, intracellular Ca^{2+} was well buffered against modest changes in external Ca^{2+}. For combined measurements of Na^+_i and Ca$^{2+}_i$, the cells were loaded with 3.5 μg/ml each of the Na$^+$ indicator, SBFI-AM, and Fluo-4-AM (both from Invitrogen), with 0.07% pluronic acid to facilitate SBFI-AM loading. Images were sequentially acquired at >1 Hz using the 340/380 nm ratio for SBFI and 490 nm for Fluo-4. KB-R7943 was from Tocris Bioscience (St. Louis, MO, USA) and, unless otherwise indicated, all other chemicals were from Sigma-Aldrich.

Combined imaging and perforated patch-clamp recordings. Microglia were plated and labeled with Fura-2-AM as described above. For perforated patch recordings the intracellular (pipette) solution contained 200 μM amphotericin (Sigma-Aldrich) and (in mM): 100 K aspartate, 40 KCl, 1 MgCl$_2$, 1 CaCl$_2$, 10 EGTA (~20 nM free Ca^{2+}), 10 HEPES, 2 MgATP, adjusted to pH 7.2 with KOH, osmolarity 280–300 mOsm. To test the effect of high intracellular Na$^+$ in perforated patch recordings, the pipette solution contained 135 mM Na aspartate instead of K aspartate. Pipettes with resistances of 4-6 MΩ were pulled from borosilicate glass (WPI, Sarasota, FL). Patch clamp recordings were made at room temperature with a Multiclamp 700A patch-clamp amplifier (Molecular Devices, Sunnyvale, CA), filtered at 5 kHz, and compensated on-line for capacitance and series resistance. Data were digitized and acquired using a Digidata 1322 board with pCLAMP ver9.0 (Molecular Devices) and were analyzed using Origin ver7.0 (OriginLabs, Northampton, MA). Liquid-liquid junction potentials were calculated using the utility in pCLAMP, confirmed by measuring the values using a 3M KCl electrode,[33] and subtracted before data analysis. After obtaining a giga-ohm seal, amphotericin caused a gradual decrease in series resistance, and when it reached <100 MΩ, experiments were begun. Fura-2 images were acquired every 2–3 s, and the excitation shutter was closed between acquisitions to prevent bleaching.

Phagocytosis-mediated respiratory burst. Microglia were plated in 96 well, black-walled plates (Corning, Acton, MA) at 5.0 x 10^4 cells/well. After 2 h, the plates were washed to remove non-adherent cells, and the microglia were cultured overnight in MEM with 2% FBS to reduce spontaneous activation.[7] At the beginning of each experiment, the medium in each well was replaced with 100 μl of bath solution containing 20 μM dihydroethidium (Invitrogen), a fluorescent indicator of reactive oxygen species.[34] After 5 min incubation at 37°C, 100 μl of medium was added to each well (final dihydroethidine concentration, 10 μM) with or without opsonized zymosan (100 μg/ml) for 1 h to stimulate the respiratory burst. Opsonized zymosan was prepared[19] by suspending zymosan (10 mg/ml) in 50% rat serum (37°C, 1 h), washing (3x in PBS) and resuspending the opsonized zymosan in PBS at 10 mg/ml.

RESULTS

Evidence for spontaneous reversal of Na$^+$/Ca^{2+} exchange in rat microglia. As a first step in analyzing the pathways of Ca^{2+} entry, we examined the effect of membrane potential on the rise in internal Ca^{2+} (Ca$^{2+}_i$) caused by depletion of Ca^{2+} stores (Fig. 1). When Fura-2AM-loaded microglia were briefly exposed to the SERCA pump inhibitor (1 μM thapsigargin) in the presence of 1 mM external Ca^{2+}, a Ca$^{2+}_i$ rise was observed in all of the thousands of cells examined. In this example, all microglia (n = 26) showed an initial Ca$^{2+}_i$ rise that is characteristic of release from internal stores and subsequent activation of store-operated Ca^{2+} (SOC) channels. We previously showed, by non-invasive imaging of membrane potential, that 55 mM external K$^+$ ([K$^+$]$_o$) depolarizes the cells from about -50 mV to about -15 mV.[26] When subsequently depolarized by elevating [K$^+$]$_o$ to 55 mM, most microglia (21/26 cells) responded with a decrease in Ca$^{2+}_i$, which rebounded when normal [K$^+$]$_o$ was restored, and then rapidly decreased when external Ca^{2+} was removed. These responses are diagnostic of store-operated Ca^{2+} entry (reviewed in refs. 35–37), which requires external Ca^{2+} and decreases when the driving force is reduced by depolarization. However, in ~10% of the optical fields, some microglia responded with a rise in Ca$^{2+}_i$ in response to depolarization. In this experiment, for example, 5/26 microglia showed a further transient Ca$^{2+}_i$ rise during the first application of the depolarizing 55 mM [K$^+$]$_o$ solution. Since this only occurred in the first response to high [K$^+$]$_o$ and the incidence was low and unpredictable, it was not feasible to assess the pharmacological profile of the underlying pathway. However, the simplest interpretation is that a second Ca^{2+} entry process was superimposed on normal store-operated Ca^{2+} entry.

The fact that this response occurred spontaneously, even though in a small proportion of cells, prompted us to study the second Ca^{2+} entry pathway in more detail. To isolate this pathway, we then omitted thapsigargin to avoid activating SOC, and used conditions that favor reversed Na$^+$/Ca^{2+} exchange. For the experiment in Figure 1B, when a strongly depolarizing bath solution was added (140 [K$^+$]$_o$, Na$^+$ free), Ca$^{2+}_i$ rapidly rose in 3/8 microglia in the optical field, showing that store depletion is not essential. All 8 cells were microglia, as confirmed by labeling with tomato lectin, as in Figure 2A. Because reversed Na$^+$/Ca^{2+} exchange can be evoked by decreasing external Na$^+$, we asked whether this procedure could produce a Ca$^{2+}_i$ rise. First, we showed that 2/20 microglia in one optical field produced a depolarization-induced Ca$^{2+}_i$ rise in 55 mM [K$^+$]$_o$ solution (Fig. 1C; only 4 cells shown). In the same two microglia, Ca$^{2+}_i$ rose when external Na$^+$ was reduced using a non-depolarizing solution; i.e., 50 mM Na$^+$ replaced by n-methyl-d-glucamine (NMDG$^+$). This experiment demonstrates a Ca$^{2+}_i$ rise evoked by reducing external Na$^+$, and an increased response by depolarizing the cells with high [K$^+$]$_o$.

Relative transcript expression of Na$^+$/Ca^{2+} exchangers in rat microglia. Data in Figure 2 show quantitative real-time RT-PCR (qRT-PCR) results comparing expression levels of the Na$^+$/Ca^{2+} exchangers, along with a membrane receptor involved in phagocytosis (CR3) and a K$^+$ channel (K$_v$1.3) that is important for the microglial respiratory burst.[24] Routine testing, like that in Figure 2A, showed that the cell cultures used in this study were 99-100% microglia. Based on their morphology[38] the untreated microglia were apparently in an 'alert' state, with most cells having long processes and amoeboid uropods. Phagocytic microglia are rod-shaped or nearly spherical.[28] The relative order of mRNA expression for the Na$^+$/Ca^{2+} exchangers was: NCX1 > NCX3 > NCX2, where '>' denotes a significant difference from the preceding gene (p < 0.05). No significant changes were detected following a 1 h treatment with opsonized zymosan to stimulate phagocytosis and the respiratory
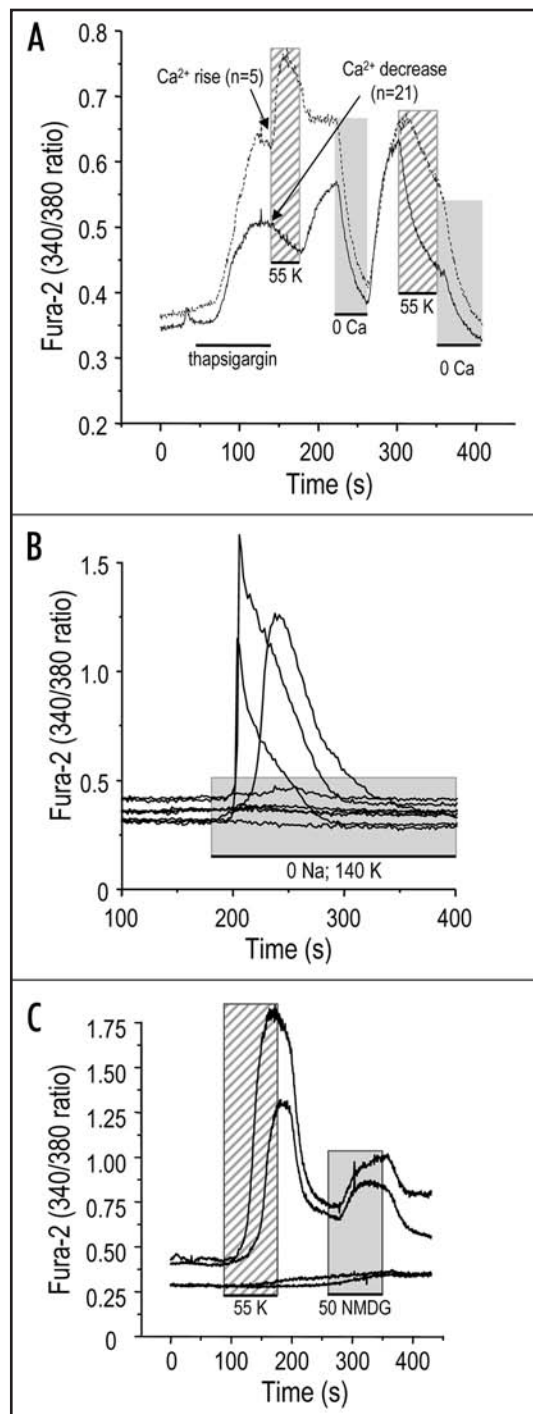
Figure 1. (Left) Evidence for spontaneous reversal of Na$^+$/Ca^{2+} exchange in rat microglia. In this, and all subsequent figures, the Fura-2 ratio indicates changes in intracellular Ca^{2+} (Ca$^{2+}_i$), a horizontal line shows the period when a pharmacological agent is present, and altered bath solutions are shown as pale-coloured boxes. Unless otherwise indicated, the bath contained standard solution (see Methods). (A) Two types of Ca$^{2+}_i$ rise can occur and show opposite responses to depolarization. In this experiment, Fura-2 loaded microglia were treated with the SERCA pump inhibitor, thapsigargin (1 μM, ~100 s) to deplete intracellular Ca^{2+} stores, while cells were exposed to standard bath solution containing (in mM): 1 Ca^{2+}, 135 Na$^+$, 5 K$^+$ (see Methods). During the plateau phase, a moderately depolarizing high external K$^+$ ([K$^+$]$_o$) solution was perfused in; i.e., 50 mM Na$^+$ replaced by K$^+$ (total [K$^+$]$_o$ 55 mM). The first time [K$^+$]$_o$ was elevated, Ca$^{2+}_i$ decreased in 21/26 microglia (solid trace is average response), but rose in 5/26 cells (dotted trace). Subsequent applications of either Ca^{2+} free or high [K$^+$]$_o$ solutions evoked a Ca$^{2+}_i$ decrease in all microglia. (B) A depolarization-induced Ca$^{2+}_i$ rise can be seen without depleting the Ca^{2+} stores; i.e., without thapsigargin. When standard bath solution was substituted with a strongly depolarizing solution ([K$^+$]$_o$ 140 mM, no Na$^+$) Ca$^{2+}_i$ increased in 3/8 microglial cells in the field. (C) The Ca$^{2+}_i$ rise is enhanced by, but does not require depolarization. When standard bath solution was replaced with the moderately depolarizing 55 mM [K$^+$]$_o$ solution, 2 cells responded with a large Ca$^{2+}_i$ rise, which decreased rapidly when the standard bath solution was restored. The other 18 cells in the field did not respond (for clarity, only 2 non-responding cells are shown). A smaller Ca$^{2+}_i$ rise in the same 2 cells occurred when a non-depolarizing bath solution with reduced Na$^+$ was perfused in (50 mM Na$^+$ replaced with NMDG$^+$).
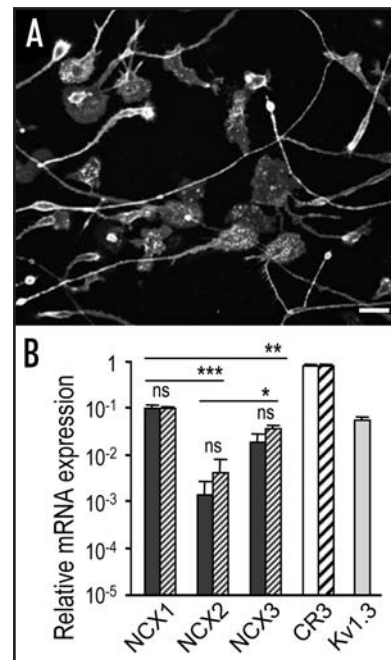

Figure 2. Relative transcript expression of Na$^+$/Ca^{2+} exchangers (*Slc8a1-3*) in rat microglia. (A) A typical culture of rat microglial cells used for quantitative real-time RT-PCR (qRT-PCR). Cells were labeled with FITC-conjugated tomato lectin (scale bar, 20 μm). (B) Relative mRNA expression was monitored by qRT-PCR, and standardized to the housekeeping gene, HPRT-1 (set to 1.0). Comparisons were made between unstimulated microglia (closed bars) and microglia after exposure for 1 h to opsonized zymosan (hatched bars). Values shown are mean ± SEM from 4 mRNA preparations made from separate batches of microglia isolated from different rat litters. Statistical differences were assessed with one way ANOVA, followed by Tukey's test for multiple comparisons, and are indicated as *p < 0.05, **p < 0.01, ***p < 0.001.

burst (see Fig. 7 for further explanation). Overall, there was a nearly 100-fold difference between NCX1 and NCX2 expression, and the NCX1 level was ~10% as high as complement receptor 3 (CR3) and the housekeeping gene (HPRT-1). K$_v$1.3 expression was also relatively high, which is interesting because it not only contributes to functions of activated microglia,[24,39] but it likely provides charge compensation for the depolarizing influence of Ca^{2+} entry, and thus maintains the Ca^{2+} driving force.[24] A useful calculation that relates the mRNA level to functional protein can be made for K$_v$1.3; i.e., the number of active K$_v$1.3 channels is about 500–1000/cell, estimated by dividing the whole-cell Kv1.3 conductance (5–10 nS)[26] by the single channel K$_v$1.3 conductance (~10 pS).[40]
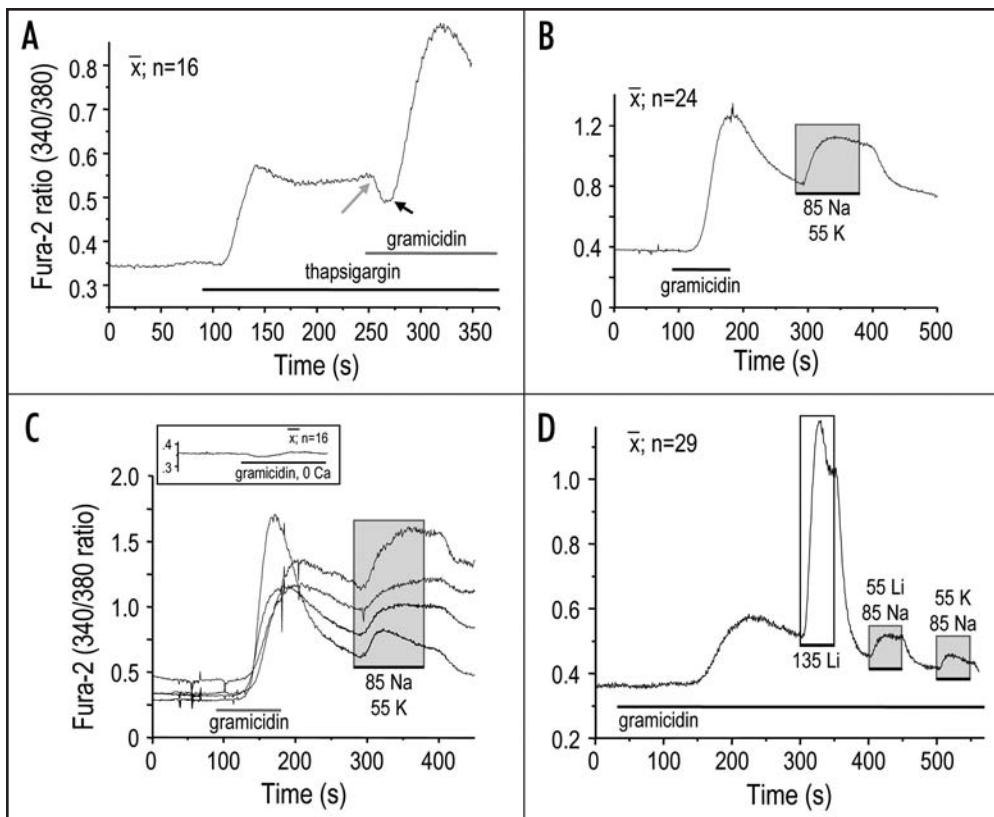
Figure 3. Properties of reversed Na$^+$/Ca^{2+} exchange revealed using the ionophore, gramicidin. (A) Ca$^{2+}_i$ rises through separate storeoperated and gramicidin-induced pathways. In standard bath solution (as in Fig. 1A), store operated Ca^{2+} entry was evoked by 1 μM thapsigargin. Subsequent addition of 1 μM gramicidin caused a small transient decrease (grey arrow) followed by a larger rise in Ca$^{2+}_i$ (black arrow). The trace is the average of 16 cells, and all cells showed similar responses. (B and C) The gramicidin-induced Ca$^{2+}_i$ rise requires external Ca^{2+} but not store depletion. Adding 1 μM gramicidin in standard bath solution caused a substantial Ca$^{2+}_i$ rise (within ~1 min), which slowly decreased when the ionophore was washed out of the bath. A second Ca^{2+} rise was evoked when the cells were subsequently superfused with a depolarizing reduced Na$^+$ solution (85 Na$^+$, 55 K$^+$). (B) Average of 24 cells. (C) 4 of the 24 cells. Inset (average of 16 cells; same amplitude and time scales) showing no Ca$^{2+}_i$ rise when 1 μM gramicidin was added in a Ca^{2+}-free bath solution. (D) External Li$^+$ does not substitute for external Na$^+$. The Ca$^{2+}_i$ rise evoked by gramicidin in standard bath solution was greatly increased when external Na$^+$ was completely replaced by Li$^+$ (135 Li$^+$, 0 Na$^+$). Partial Na$^+$ replacement by either Li$^+$ or K$^+$ evoked smaller responses.

Properties of reversed Na$^+$/Ca^{2+} exchange revealed using the ionophore, gramicidin. The unexpected Ca^{2+} rises observed in unstimulated microglia that were consistent with reversed Na$^+$/Ca^{2+} exchange (Fig. 1), prompted us to design experimental conditions to reliably activate the transporter and facilitate more detailed studies of its properties. We exploited the expectation that the direction and magnitude of Na$^+$/Ca^{2+} exchange will depend on both ion gradients, and on the membrane potential, as follows. Under normal conditions, Na$^+$/Ca^{2+} exchangers mediate Na$^+$ influx and Ca^{2+} efflux. They are electrogenic, exchanging 3 Na$^+$ ions for each Ca^{2+} ion, and their reversal potentials can be calculated from: $E_{NCX} = 3E_{Na} - 2E_{Ca}$, where E_{Na} and E_{Ca} are the Nernst potentials for Na$^+$ and Ca^{2+}.[41] First, we calculated the predicted reversal potential under physiologically relevant conditions. Reported values for intracellular Na$^+$ (Na^+_i) in microglia range from 2–7 mM under resting conditions, to 5–11 mM after stimulation (e.g., with glycine).[42] To calculate E_{NCX}, we first converted concentrations (c) to activities (a_{ion}) using the formula: $a_{ion} = f_{ion}c_{ion}$ where log $f_{ion} = (-0.51z^2\sqrt{I})\_(1+\sqrt{I})$, and I is ionic strength. Setting Na^+_i at 5 mM, and Ca$^{2+}_i$ at 70 nM (the

mean resting value determined by calibrating the Fura-2 signal), and taking the bath concentrations of 135 mM Na$^+$ and 1 mM Ca^{2+}, the calculated E_{NCX} is +9 mV. But, if intracellular Na$^+$ rises to as little as 11 mM, E_{NCX} becomes -52 mV in the standard bath. Furthermore, if external Na$^+$ is reduced to 85 mM (as is frequently used experimentally; see Fig. 1), then E_{NCX} will become -26 mV if Na^+_i is 5 mM, and -87 mV if Na^+_i is 11 mM. Using a voltage-sensitive dye, we measured the resting potential to be about -50 mV;[26] hence, it should be easy to reverse the driving force and evoke Ca^{2+} entry if the membrane potential becomes depolarized, or the Na$^+$ gradient is reduced by increasing Na^+_i or experimentally reducing external Na$^+$. It is thus not surprising that Ca^{2+} entry occurred in some microglia (Fig. 1) when they were moderately depolarized (55 mM K^+_o) or external Na$^+$ was reduced to 85 mM.

Experiments shown in Figures 3, 4 and 6 exploit the ionophore, gramicidin, and in order to interpret the results it is first necessary to consider its properties. Gramicidin forms channels that are permeable to K$^+$ and Na$^+$;[43] thus, it rapidly depolarizes cells and more slowly dissipates the transmembrane Na$^+$ and K$^+$ gradients. The rise in internal Na$^+$ should reverse Na$^+$/Ca^{2+} exchangers and promote Ca^{2+} entry. In order to observe the onset of these effects, gramicidin was added after the Ca^{2+} imaging recordings were begun.

Because gramicidin is hydrophobic, the stock solution (1 mM in DMSO) was vortexed and immediately added to the superfusion solution to achieve a final concentration of 1 μM (no precipitates were seen). The membrane:water partition coefficient of gramicidin is > 1; thus, it accumulates in the membrane. Upon washing, it slowly leaches out and the amount remaining at any time is unknown. Two recordings are shown with washing (Fig. 2B and C); otherwise, gramicidin was left in the bath to reduce the experimental complexity while maintaining a pathway for Na$^+$ influx. To raise internal Na$^+$, we found the gramicidin method preferable to using receptor-mediated pathways that would evoke direct Ca^{2+} entry (if ionotropic), or Ca^{2+} release from stores (if metabotropic), which would activate store-operated channels (SOCs) and confound attempts to isolate the Na$^+$/Ca^{2+} exchange.

In the first experiment (Fig. 3A), we evoked store-operated Ca^{2+} entry with thapsigargin and then applied gramicidin to fully depolarize the cells. As expected, the immediate response to gramicidin was a decrease in Ca$^{2+}_i$, consistent with a depolarization-induced decrease in driving force for Ca^{2+} entry. This was soon followed by a large rise

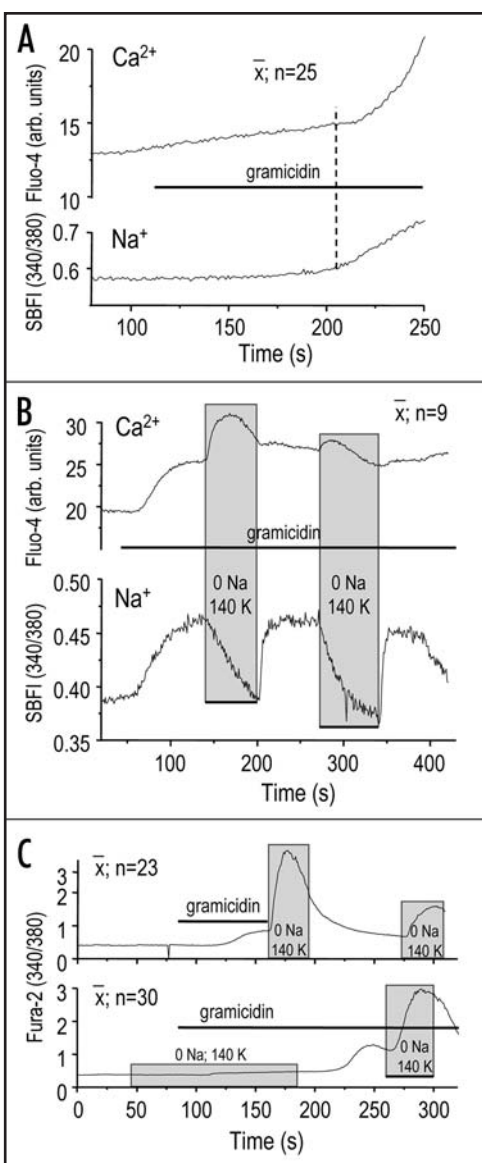Figure 4. Elevated internal Na$^+$ evokes a Ca$^{2+}_i$ rise through reversed Na$^+$/Ca^{2+} exchange. (A and B) Changes in intracellular Na$^+$ correlate with Ca^{2+} entry. Simultaneous imaging of intracellular Ca^{2+} and Na$^+$ in microglia loaded with Fluo-4-AM (490 nm excitation) and SBFI-AM (ratio imaged at 340/380 nm excitation). In standard bath solution, 1 μM gramicidin elicited a rise in Na$^+$ and then Ca^{2+}. (A) Is on an expanded time scale to show the inflection point in the Na$^+$ rise (dashed line). Removing external Na$^+$ (B) evoked a further increase in Ca^{2+}. (C) The Ca$^{2+}_i$ rise requires intracellular Na$^+$. Fura-2 ratio imaging of intracellular Ca^{2+}. Upper panel: Gramicidin (1 μM) evoked a Ca^{2+} rise that was greatly enhanced by removing external Na$^+$. Lower panel: When first added in a Na$^+$-free bath solution, gramicidin did not evoke a Ca^{2+} rise. After external Na$^+$ was restored, the normal responses occurred (similar to the first responses in the upper panel).

in Ca$^{2+}_i$, as expected for reversed Na$^+$/Ca^{2+} exchange resulting from depolarization combined with a rise in intracellular Na$^+$. Importantly, experiments in Figure 3B–D show that the gramicidin-induced Ca$^{2+}_i$ rise does not require depletion of intracellular Ca^{2+} stores and activation of store-operated channels. That is, adding gramicidin alone caused a substantial Ca$^{2+}_i$ rise (Fig. 3B), and although the individual cell responses varied in amplitude (Fig. 3C) they were qualitatively similar in all cells examined. Changes in Ca^{2+} concentration were

calculated (from Fura-2 signals) in several such experiments: in standard bath solution, Ca$^{2+}_i$ increased from 68 ± 5 nM to 285 ± 18 nM at 100 s after gramicidin application (n = 115 cells). This Ca$^{2+}_i$ rise required influx, but not release from internal stores, since it was fully prevented by removing extracellular Ca^{2+} (inset in Fig. 3C). Importantly, exposure to gramicidin rendered all microglia responsive, such that a subsequent exposure to a depolarizing solution with reduced external Na$^+$ (Fig. 3B and C) evoked a Ca$^{2+}_i$ rise in all cells examined (> 200 cells).

There was a delay after adding gramicidin until a rise in Ca$^{2+}_i$ was seen (~30 sec to > 60 sec), which reflects several processes; exchanging the bath solution (~10 sec), incorporation and accumulation of gramicidin in cell membranes, and diffusion-mediated run-down of the ion gradients. The latter two processes will be affected by activity of pumps and other transporters and by cell surface-to-volume ratio, which is highly variable for microglia that range from highly ramified 'resting' cells, to 'amoeboid' cells that can bear long processes, to rounded up 'fully activated' cells. Others have observed a relatively slow equilibration of internal Na$^+$ and a delayed rise in Ca$^{2+}_i$ after adding gramicidin, as much as 3–4 min.[44] A more direct study using gramicidin to calibrate the Na$^+$-sensitive dye, SBFI, showed a variable time course. When external Na$^+$ was reduced the gradient did not collapse immediately, despite inhibiting the Na$^+$/K$^+$ ATPase with ouabain.[45] Alternatively, some studies preincubate with gramicidin for several minutes to allow the cells to load with Na$^+$ before recording rapid responses to changes in extracellular ions.[46] The slow dissipation of the Na$^+$ gradient is also consistent with the experiment in Figure 3D. When external Na$^+$ was completely replaced with Li$^+$, there was an immediate, large rise in Ca$^{2+}_i$ due to the removal of Na$^+$. This was followed within seconds by a relaxation of the Ca$^{2+}_i$ signal in all cells examined. This time course was entirely consistent with Li$^+$ influx and Na$^+$ efflux through gramicidin channels, and the failure of Li$^+$ to support the reversed mode of the Na$^+$/Ca^{2+} exchanger.[41] We did not examine the time course of the relaxation using longer experiments with Li$^+$, but an earlier study[44] applied gramicidin for > 10 min before testing Li$^+$ substitution. As expected, the Ca$^{2+}_i$ rise in our experiment was smaller if Na$^+$ was reduced to 85 mM rather than 0 mM. Together, all results in Figure 3 are consistent with reversal of a Na$^+$/Ca^{2+} exchanger.

A rise in internal Na$^+$ evokes reversed-mode Na$^+$/Ca^{2+} exchange. Next, we directly examined the rate of rise in cytoplasmic Na$^+$ in response to gramicidin and demonstrate that Ca^{2+} influx can be evoked in microglia by reducing the Na$^+$ gradient. Intracellular Na$^+$ was imaged with SBFI, and Fluo-4 was used to simultaneously image Ca$^{2+}_i$ because its excitation and emission wavelengths allow dual imaging. Figure 4A demonstrates that both intracellular ions rise and, as can be seen from the inflection points, the increase in intracellular Na$^+$ (beginning after ~85 sec in this example) preceded the Ca$^{2+}_i$ rise. NB: The slow drift in Ca^{2+} signal occurs because Fluo-4 is not a ratiometric dye. The role of the Na$^+$ gradient was confirmed in Figure 4B. When gramicidin was first perfused into the bath, intracellular Na$^+$ began to rise after a delay (~30 sec) and approached a plateau after >1 min. Removing external Na$^+$ evoked a rapid rise in Ca$^{2+}_i$ and slower decline in internal Na$^+$, which is consistent with reversed Na$^+$/Ca^{2+} exchange. Then, as expected after allowing time for gramicidin to accumulate in the cell membranes, the subsequent rises in internal Na$^+$ were much more rapid and reflected changes in external Na$^+$. Results in Figure 4C show that the Ca$^{2+}_i$ rise required
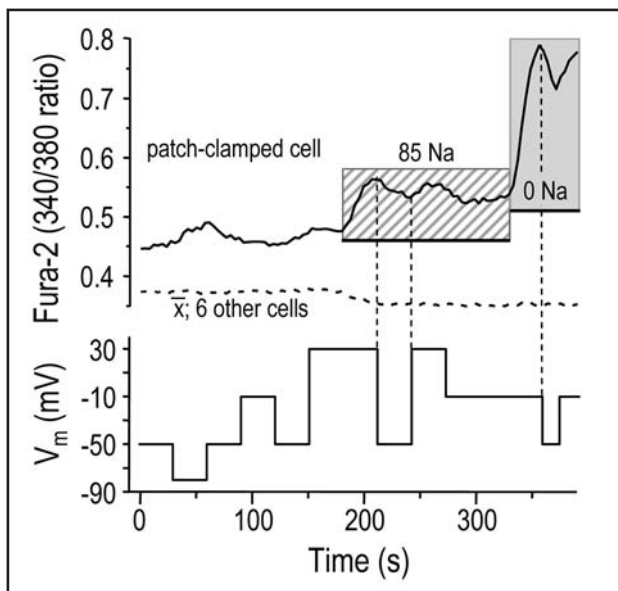
Figure 5. Voltage-dependence of Ca^{2+} entry through reversed-mode Na$^+$/Ca^{2+} exchange. Amphotericin-mediated perforated patch recordings (explained in Results) were combined with simultaneous Ca^{2+} imaging of Fura-2 AM-loaded cells. To increase intracellular Na$^+$ in the patch-clamped cell, the pipette solution contained 135 mM Na$^+$. Changes in intracellular Ca^{2+} were evoked by voltage steps (to −80, −50, −10 and +30 mV; lower panel). First, the bath contained standard solution, then external Na$^+$ was reduced to 85 mM, and finally all external Na$^+$ was replaced by K$^+$. Vertical dashed lines show selected voltage changes aligned with Ca^{2+} responses.

Figure 6. Pharmacological inhibition of the gramicidin-evoked Na$^+$/Ca^{2+} exchange. (A) Upper panel: Control recording showing the normal responses to gramicidin and removing external Na$^+$ (similar to Fig. 4C). Lower panel: An inhibitor of reversed Na$^+$/Ca^{2+} exchange, KB-R7943 (10 μM) prevented the Ca$^{2+}_i$ rise in response to removing external Na$^+$. (B) The L-type Ca^{2+} channel blocker, 5 μM nifedipine, had no effect: Ca$^{2+}_i$ rose normally in response to gramicidin and to reducing external Na$^+$.

reversal of the Na$^+$/Ca^{2+} exchanger, and was not a direct result of removing external Na$^+$. When gramicidin was added in the absence of external Na$^+$ (lower panel), removing external Na$^+$ did not evoke a Ca$^{2+}_i$ change. This is most likely because internal Na$^+$ was depleted by efflux through the Na$^+$ permeable gramicidin channels (as in Fig. 4B). However, after allowing time for internal Na$^+$ to be replenished in standard bath solution, normal Ca$^{2+}_i$ responses were restored. Note that in control experiments with normal bath Na$^+$ (upper panel); gramicidin produced the usual responses to removal of external Na$^+$ in cells from the same batches.

The voltage-dependence of Ca^{2+} entry mediated by Na$^+$/Ca^{2+} exchange. To directly determine the effect of membrane potential (V$_m$) on Ca^{2+} entry through reversed-mode Na$^+$/Ca^{2+} exchange, the Fura-2 signal was imaged while the membrane potential was controlled in current clamp recordings. The perforated patch configuration was used with amphotericin, which allows whole-cell recording by forming channels that are permeable to monovalent ions (Na$^+$, K$^+$, Cl$^-$) but impermeable to divalent cations.[47] Thus, in order to promote reversal of the Na$^+$/Ca^{2+} exchanger, intracellular Na$^+$ can be elevated in each patch-clamped cell using a pipette solution containing 135 mM Na$^+$. However, just as explained above for gramicidin channels, the Na$^+$ gradient will not immediately equilibrate between the pipette and cytoplasm. In addition, the pipette solution will not directly affect the intracellular Ca^{2+} concentration. In each microscope field (e.g., Fig. 5), the Ca$^{2+}_i$ response was compared between several intact microglia and a single patch-clamped cell held at -50 mV, which is about the resting potential of intact microglia.[26] With standard bath solution, hyperpolarizing and depolarizing steps evoked very small changes in internal Ca^{2+}. However, when the cell
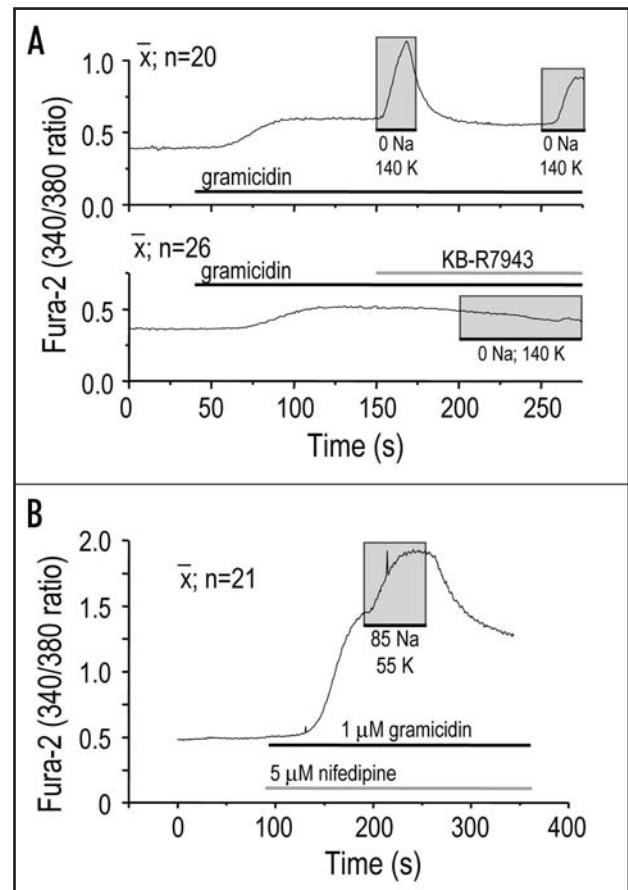
was stepped to a depolarized V$_m$, reducing external Na$^+$ to 85 mM increased the Ca$^{2+}_i$ rise (see step to +30 mV), and the Ca$^{2+}_i$ rise was even larger when external Na$^+$ was 0 mM (see step to -10 mV). With either external Na$^+$ concentration, subsequent hyperpolarizing steps reduced Ca$^{2+}_i$ from this elevated level. Similar results were observed in all 5 cells tested. These results are entirely consistent with reversed Na$^+$/Ca^{2+} exchange, and importantly, they rule out Ca^{2+} influx through Ca^{2+} channels, which does not depend on external Na$^+$, and will decrease at +30 mV owing to the reduced driving force. Note that in non-patch-clamped cells in the same optical field, Ca$^{2+}_i$ was unaffected by V$_m$, and reduced only very slightly when external Na$^+$ was reduced.

Reversed Na$^+$/Ca^{2+} exchange contributes to the phagocytosis-mediated respiratory burst. The evidence presented thus far is that reversed Na$^+$/Ca^{2+} exchange can be readily evoked in microglia under the appropriate conditions; i.e., depolarization, increased intracellular Na$^+$ or reduced external Na$^+$. Before addressing functional roles of the exchanger, it was necessary to identify a pharmacological inhibitor. KB-R7943 is a broad-spectrum NCX blocker that preferentially blocks the reversed mode of the exchangers,[48] with a reported IC$_{50}$ of ~5 μM.[48,49] First, we elicited stereotypical Ca$^{2+}_i$ rises in
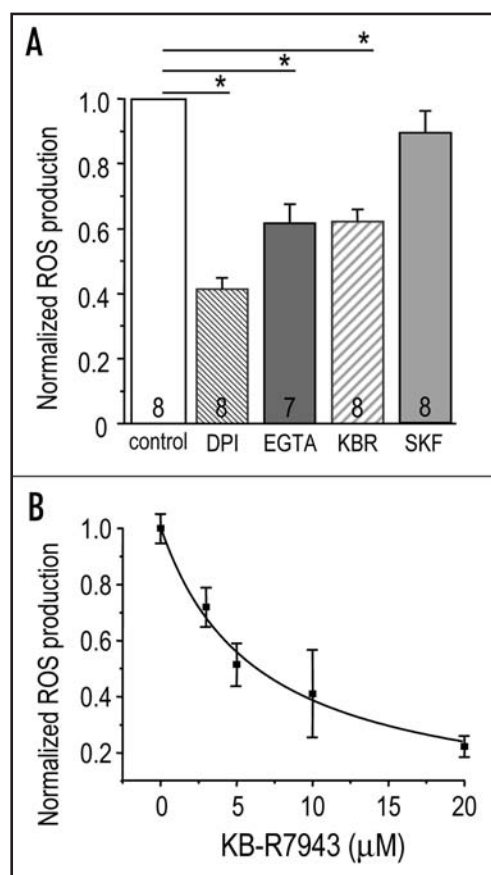
Figure 7. Role of reversed Na$^+$/Ca^{2+} exchange in the phagocytosis-mediated respiratory burst. (A) Role of Ca^{2+} entry through reversed Na$^+$/Ca^{2+} exchange. An NADPH-mediated respiratory burst was evoked in response to phagocytosis of opsonized zymosan (100 μg/ml; 1 h, 37°C), and monitored as a fluorescence increase in microglia labeled with 10 μM dihydoethidium (see Methods). After subtracting the fluorescence signal from un-stimulated cells, the signal was normalized to the value in drug-free controls. Values are mean ± SEM for the number of separate experiments indicated on each bar (*p < 0.05). When used, each of the following compounds was added to the bath at the same time as opsonized zymosan: the NADPH inhibitor, diphenylene iodonium (DPI; 200 nM); the Ca^{2+} chelator, EGTA (10 mM); and the Na$^+$/Ca^{2+} exchanger inhibitor, KB-R7943 (20 μM) (B) Dose-dependence of inhibition by KB-R7943 (mean ± SEM, n = 3). The respiratory burst was monitored at different concentrations of KB-R7943. A curve was fit to: percent block = 1/[1+(IC$_{50}$/[KBR])], yielding an IC$_{50}$ of 5.0 μM.

control recordings from several cell batches (Fig. 6A, upper panel), and then showed that 10 μM KB-R7943 prevented the response to removing external Na$^+$ (lower panel) in aliquots from the same cell batches. It has been suggested that microglia express functional voltage-dependent L-type Ca^{2+}. Results above (Fig. 5) appeared to rule out a contribution of Ca^{2+} channels to the Ca$^{2+}_i$ rise when intracellular Na$^+$ is elevated. In Figure 6B, a contribution of L-type Ca^{2+} channels is ruled out because the typical Ca$^{2+}_i$ responses to gramicidin were unaffected by nifedipine (5 μM shown or 100 μM not shown).

To address the physiological importance of Na$^+$/Ca^{2+} exchange-mediated Ca^{2+} influx, we asked whether it plays a role in the respiratory burst, which can render activated microglia neurotoxic.[21,24] Phagocytosis was stimulated using opsonized zymosan, and the ensuing respiratory burst was monitored as superoxide

production, and shown to be mediated by NADPH-oxidase, because it was inhibited by diphenylene iodonium (DPI). External Ca^{2+} was required, since superoxide production was inhibited by chelating Ca^{2+} in the bath with 10 mM EGTA. Most importantly, KB-R7943 dose-dependently reduced the respiratory burst, with an IC$_{50}$ of ~5 μM (Fig. 7B); the same as the published value for inhibiting Na$^+$/Ca^{2+} exchangers (see above). KB-R7943 has been reported to inhibit store-operated Ca^{2+} (SOC) channels; however, this side effect was ruled out because the SOC inhibitor, SKF-96365, had no effect (Fig. 7A). Finally, KB-R7943 has been reported to displace some L-type Ca^{2+} channel blockers (verapamil, diltiazem; but not the dihydropyridine, PN200-100) from binding sites in rat cerebral cortex.[48] However, we ruled out an involvement of L-type Ca^{2+} channels in the Ca^{2+} rise (Fig. 6B), and found that the respiratory burst was not reduced by nifedipine. That is, superoxide production was 96.9 ± 8.0% of the control value with 5 μM and 94.9 ± 6.9% with 25 μM nifedipine (p > 0.2; n = 3 cultures). KB-R7943 does not inhibit several other ion transport molecules that are potentially involved in the respiratory burst in microglia; such as, Na$^+$/H$^+$ exchanger, Na$^+$/K$^+$ ATPase or Ca^{2+} ATPases.[48]

DISCUSSION

This study provides direct evidence that Ca^{2+} entry by reversed Na$^+$/Ca^{2+} exchange can occur under normal conditions and can contribute to microglial activation. Using single-cell Ca^{2+} imaging and perforated patch-clamp recording, we demonstrated the salient features of this Na$^+$/Ca^{2+} exchange. The significant findings are: (i) The rise in intracellular Ca^{2+} (Ca$^{2+}_i$) was abolished by removing external Ca^{2+}, which demonstrates that the source is Ca^{2+} influx, not internal release. In addition, this Ca^{2+} influx pathway did not require depletion of Ca^{2+} stores, and thus differs from store-operated Ca^{2+} channels. (ii) Ca^{2+} entry through reversed Na$^+$/Ca^{2+} exchange was enhanced by depolarization, which potentially resolves discrepancies in the literature concerning the existence of depolarization-activated L-type Ca^{2+} channels in microglia. (iii) Conditions were delineated under which reversed Na$^+$/Ca^{2+} exchange was induced in all of the thousands of microglia examined. This occurred when they were loaded with Na$^+$ using the cationophore, gramicidin (confirmed with a Na$^+$-sensitive dye), or when some extracellular Na$^+$ was replaced with a non-transported cation, or when the microglia were moderately depolarized. (iv) Another key observation, which is consistent with reversed Na$^+$/Ca^{2+} exchange, is the link between efflux of internal Na$^+$ and influx of external Ca^{2+}. That is, there was a time lag during which internal Na$^+$ rose, and it preceded the Ca$^{2+}_i$ rise, which was also prevented if intracellular Na$^+$ was depleted. (v) The relative transcript levels of Na$^+$/Ca^{2+} exchangers was NCX1 > NCX3 > NCX2, and was unaltered during the time required for the microglia to phagocytose opsonized zymosan. (vi) Finally, Ca^{2+} influx through reversed Na$^+$/Ca^{2+} exchange contributed to a generally neurotoxic microglia function, the NADPH-mediated respiratory burst that accompanies phagocytosis. That is, Ca^{2+} influx through this pathway and phagocytosis were reduced by the same concentrations of the Na$^+$/Ca^{2+} exchanger inhibitor, KB-R7943.

Based on these properties, Ca^{2+} entry through reversed Na$^+$/Ca^{2+} exchange will likely be most important under pathological conditions that favor microglia depolarization or an elevation in either internal Na$^+$ or external K$^+$. Interestingly, in a small proportion

of cultured microglial cells we found reversed Na$^+$/Ca^{2+} exchange without any manipulations. This observation may indicate that some microglia have higher initial Na$^+$ levels, depolarized membrane potentials or both. Of note, the likelihood of observing reversed Na$^+$/Ca^{2+} exchange activity and the resulting rise in intracellular Ca^{2+} were dramatically increased when internal Na$^+$ was elevated. Especially under pathological conditions, several pathways can potentially cause a rise in cytoplasmic Na$^+$. For instance, microglia have Na$^+$-permeable ion channels, including non-selective cation channels,[42] and ionotropic purinergic receptors[50-52] (reviewed in refs. 15 and 53) that can be activated by ATP release from damaged cells. Microglia also robustly express functional TRPM7 channels,[54] which can conduct large inward monovalent currents; e.g., when extracellular pH is reduced to levels that have been observed during tissue injury, ischemia, repetitive nerve activity or seizures.[55] In addition, activated microglia express high levels of Na$^+$/glutamate co-transporters[56] which, in astrocytes, cause large glutamate-induced elevations in internal Na$^+$. Extracellular glycine, which increases in ischemia, neurotrauma and epilepsy, elevates internal Na$^+$ in microglia through Na$^+$-coupled neutral amino acid transporters.[42] In astrocytes, ischemia and reperfusion dramatically increase internal Na$^+$ through a Na$^+$/K$^+$/Cl$^-$ cotransporter,[57,58] and a similar mechanism might exist in microglia. Thus, there are numerous conditions under which Na$^+$ influx should elevate internal Na$^+$ in microglia, causing reversal of Na$^+$/Ca^{2+} exchange and consequent Ca^{2+} entry (see Results for sample calculations). Furthermore, reversal of Na$^+$/Ca^{2+} exchange will be facilitated by some changes in extracellular ions that occur under a variety of pathological conditions. Changes in extracellular K$^+$ [K$^+$]$_o$ are especially important because they can affect the membrane potential. After brain ischemia, [K$^+$]$_o$ rises and [Na$^+$]$_o$ falls to levels comparable to those used in the present study; e.g., after 15 min of ischemia [K$^+$]$_o$ rises to 42 mM and [Na$^+$]$_o$ falls to 64 mM.[59]

Reversed Na$^+$/Ca^{2+} exchange is relevant to a broad range of CNS pathologies. It appears to mediate 'Ca^{2+}-paradox injury', which is delayed cell death due to a persistent rise in internal Ca^{2+} after cells are exposed to Ca^{2+}-free solutions, then reperfused with normal Ca^{2+}.[48] This process is often considered to be an in vitro model of cerebral ischemia/reperfusion injury because a similar decrease, followed by an increase in external Ca^{2+} has been seen after stroke.[60] There are two families of Na$^+$/Ca^{2+} exchanger genes with several members each; the strictly Na$^+$/Ca^{2+} dependent, *SLC8A*/NCX family (usually called *Slc8a* in rodents) and the K$^+$ dependent *SLC24*/NCKX family. Both families are expressed in the brain but their cellular distribution has not been fully characterized, and the precise gene (or genes) involved in brain injury is not known. All three members of the *Slc8a1-3*/NCX1-3 family are found in microglia (ref. 48 and present study), and the most highly expressed, *Slc8a1*/NCX1, is an important Ca^{2+} transporter in most cells (reviewed in ref. 61). Although we did not detect a change in their expression after inducing phagocytosis for one hour; pathological conditions, other stimuli and those acting over longer periods might affect exchanger expression. For instance, both NCX expression and Ca^{2+} signaling were found to be transiently up-regulated after treatment with IFNγ,[62] a cytokine implicated in CNS pathologies such as stroke. In future, it would be interesting to determine if TNFα and IL1β, which evoke chronic Ca^{2+} elevations in microglia (reviewed in ref. 16) also up-regulate *Slc8a1*/NCX expression or activity. We had hoped to

use siRNA-mediated knockdown to identify the specific NCX gene that mediates the reversed Na$^+$/Ca^{2+} exchange. If successful, this approach could also be used to assess roles of identified *Slc8a1*/NCX genes in microglia-mediated neurotoxicity, as we have previously done for microglial K$^+$ channels.[24,25] However, we have found that siRNA mediated knockdown is extremely difficult and inefficient in primary microglial cells, and most transfection or infection treatments were toxic (unpublished results).

Numerous studies implicate oxygen free radicals in microglia-mediated neuron damage after stroke (reviewed in ref. 63). How, specifically, might reversed Na$^+$/Ca^{2+} exchange contribute to the respiratory burst? Ionic requirements for the NADPH-mediated respiratory burst in phagocytes are complex but worth considering when comparing the present results with previous work. Many studies use a phorbol ester to evoke a respiratory burst; however, in bypassing the phagocytosis receptors, downstream signaling mechanisms will likely be compromised. An important methodological difference is that in the present study, the respiratory burst was a consequence of phagocytosis. Under these conditions, external Ca^{2+} was required for superoxide production, and we provide the first evidence that reversed Na$^+$/Ca^{2+} exchange contributes to this respiratory burst in microglia. During the respiratory burst, depolarization and a rise in internal Na$^+$ have been observed,[64] both of which should promote reversal of Na$^+$/Ca^{2+} exchange and consequent Ca^{2+} entry. The voltage dependence of reversed Na$^+$/Ca^{2+} exchange shown in the present study might explain earlier observations that the phorbol ester-induced respiratory burst is potentiated by high external K$^+$,[20,22] which should depolarize the cells.

A second consideration is that in order to produce a respiratory burst, NADPH is converted to NADP$^+$ and H$^+$, electrons are released and they combine with O$_2$ to form extracellular O$_2^-$ (superoxide).[65] In principle, the electron efflux could depolarize the cell sufficiently to reverse Na$^+$/Ca^{2+} exchange without a rise in internal Na$^+$. Concurrent with NADPH activation, H$^+$ is released to acidify the phagosomes. If activated at the plasma membrane, Na$^+$/H$^+$ exchangers will promote Na$^+$ influx while extruding H$^+$.[66,67] One potential mechanism to compensate for depolarization and maintain the large driving force for electron efflux that drives NADPH oxidase, is to promote K$^+$ efflux through ion channels. Such a mechanism is consistent with the dramatically reduced respiratory burst when voltage-dependent (K$_v$) or Ca^{2+}-dependent (SK) channels are blocked in microglia.[22,24,68] In addition, Cl$^-$ influx through anion channels[28,69] could help counteract the depolarization resulting from electron efflux. We recently showed that anion channels are major determinants of the membrane potential in microglia[26] and thus, should affect Ca^{2+} entry, and also contribute to phagocytosis.[28] We recognize that quantitative and qualitative differences in the predominant ionic pathways might exist between different cell types and might also depend on the stimulus used. When the much larger respiratory burst is activated by phorbol esters in eosinophils or neutrophils, efflux through an H$^+$ selective channel appears to counteract the depolarization and remove excess internal H$^+$.[66]

Based on the role of reversed Na$^+$/Ca^{2+} exchange in elevating Ca^{2+} and activating astrocytes, a potent inhibitor, SEA0400, was tested and found to improve the outcome in a rat model of transient ischemic stroke.[48] The present results showing a role for reversed Na$^+$/Ca^{2+} exchange in the phagocytosis-mediated respiratory burst in

microglia, supports testing specific inhibitors in models of a variety of CNS pathologies that involve release of potentially toxic free radicals from microglia.

References

1. Aloisi F. Immune function of microglia. Glia 2001; 36:165-79.
2. Basu A, Krady JK, Levison SW. Interleukin-1: A master regulator of neuroinflammation. J Neurosci Res 2004; 78:151-6.
3. Block ML, Zecca L, Hong JS. Microglia-mediated neurotoxicity: Uncovering the molecular mechanisms. Nature Rev 2007; 8:57-69.
4. Hanisch UK. Microglia as a source and target of cytokines. Glia 2002; 40:140-155.
5. Inoue K. The function of microglia through purinergic receptors: Neuropathic pain and cytokine release. Pharmacol Ther 2006; 109:210-26.
6. Rotshenker S. Microglia and macrophage activation and the regulation of complement-receptor-3 (CR3/MAC-1)-mediated myelin phagocytosis in injury and disease. J Mol Neurosci 2003; 21:65-72.
7. Schlichter LC, Khanna R. Potassium channels and proliferation of neuroimmune cells. In: Rouzaire-Dubois B, Benoit E, Dubois JM, eds. Ion Channels and Physiopathologies of Nerve Conduction And Cell Proliferation. Trivandrum, Kerala, India: Research Signpost, 2002:121-51.
8. Stoll G, Jander S, Schroeter M. Detrimental and beneficial effects of injury-induced inflammation and cytokine expression in the nervous system. Adv Exp Med Biol 2002; 513:87-113.
9. Streit WJ, Conde JR, Fendrick SE, Flanary BE, Mariani CL. Role of microglia in the central nervous system's immune response. Neurol Res 2005; 27:685-91.
10. Streit WJ, Mrak RE, Griffin WS. Microglia and neuroinflammation: A pathological perspective. J Neuroinflam 2004; 1:14.
11. Town T, Nikolic V, Tan J. The microglial "activation" continuum: From innate to adaptive responses. J Neuroinflam 2005; 2:24.
12. Vilhardt F. Microglia: Phagocyte and glia cell. Int J Biochem Cell Biol 2005; 37:17-21.
13. Inoue K. Microglial activation by purines and pyrimidines. Glia 2002; 40:156-63.
14. Moller T, Kann O, Verkhratsky A, Kettenmann H. Activation of mouse microglial cells affects P2 receptor signaling. Brain Res 2000; 853:49-59.
15. McLarnon JG. Purinergic mediated changes in Ca²⁺ mobilization and functional responses in microglia: Effects of low levels of ATP. J Neurosci Res 2005; 81:349-56.
16. Farber K, Kettenmann H. Physiology of microglial cells. Brain Res Brain Res Rev 2005; 48:133-43.
17. Farber K, Kettenmann H. Functional role of calcium signals for microglial function. Glia 2006; 54:656-65.
18. Matsuda T, Nagano T, Takemura M, Baba A. Topics on the Na⁺/Ca²⁺ exchanger: Responses of Na⁺/Ca²⁺ exchanger to interferon-gamma and nitric oxide in cultured microglia. J Pharmacol Sci 2006; 102:22-6.
19. Colton CA, Gilbert DL. Production of superoxide anions by a CNS macrophage, the microglia. FEBS Lett 1987; 223:284-8.
20. Colton CA, Jia M, Li MX, Gilbert DL. K⁺ modulation of microglial superoxide production: Involvement of voltage-gated Ca²⁺ channels. Am J Physiol 1994; 266:C1650-5.
21. Qin LY, Liu YX, Wang TG, Wei SJ, Block ML, Wilson B, Liu B, Hong JS. NADPH oxidase mediates lipopolysaccharide-induced neurotoxicity and proinflammatory gene expression in activated microglia. J Biol Chem 2004; 279:1415-21.
22. Spranger M, Kiprianova I, Krempien S, Schwab S. Reoxygenation increases the release of reactive oxygen intermediates in murine microglia. J Cereb Blood Flow Metab 1998; 18:670-4.
23. Anderson ME. Calmodulin kinase and L-type calcium channels; a recipe for arrhythmias? Trends Cardiovasc Med 2004; 14:152-61.
24. Fordyce CB, Jagasia R, Zhu X, Schlichter LC. Microglia Kv1.3 channels contribute to their ability to kill neurons. J Neurosci 2005; 25:7139-49.
25. Kaushal V, Koeberle PD, Wang Y, Schlichter LC. The Ca²⁺-activated K⁺ channel KCNN4/KCa3.1 contributes to microglia activation and nitric oxide-dependent neurodegeneration. J Neurosci 2007; 27:234-44.
26. Newell EW, Schlichter LC. Integration of K⁺ and Cl⁻ currents regulate steady-state and dynamic membrane potentials in cultured rat microglia. J Physiol 2005; 567:869-890.
27. Bustin SA, Nolan T. Pitfalls of quantitative real-time reverse-transcription polymerase chain reaction. J Biomol Tech 2004; 15:155-66.
28. Ducharme G, Newell EW, Pinto C, Schlichter LC. Small-conductance Cl⁻ channels contribute to volume regulation and phagocytosis in microglia. Eur J Neurosci 2007; 26:2119-30.
29. Wasserman JK, Schlichter LC. Neuron death and inflammation in a rat model of intracerebral hemorrhage: Effects of delayed minocycline treatment. Brain Res 2007; 1136:208-18.
30. Wasserman JK, Schlichter LC. Minocycline protects the blood-brain barrier and reduces edema following intracerebral hemorrhage in the rat. Exp Neurol 2007; 207:227-37.
31. Schlichter LC, Sakellaropoulos G. Intracellular Ca²⁺ signalling induced by osmotic shock in human T lymphocytes. Exp Cell Res 1994; 215:211-22.
32. Grynkiewicz G, Poenie M, Tsien RY. A new generation of Ca²⁺ indicators with greatly improved fluorescence properties. J Biol Chem 1985; 260:3440-50.
33. Barry PH, Lynch JW. Liquid junction potentials and small cell effects in patch-clamp analysis. J Membr Biol 1991; 121:101-17.
34. Haugen TS, Skjonsberg OH, Kahler H, Lyberg T. Production of oxidants in alveolar macrophages and blood leukocytes. Eur Respir J 1999; 14:1100-5.
35. Parekh AB, Putney Jr JW. Store-operated calcium channels. Physiol Rev 2005; 85:757-810.
36. Penner R, Fleig A. Store-operated calcium entry: A tough nut to CRAC. Sci STKE 2004; 2004:38.
37. Prakriya M, Lewis RS. CRAC channels: Activation, permeation, and the search for a molecular identity. Cell Calcium 2003; 33:311-21.
38. Dailey ME, Waite M. Confocal imaging of microglial cell dynamics in hippocampal slice cultures. Methods 1999; 18:222-30.
39. Kotecha SA, Schlichter LC. A Kv1.5 to Kv1.3 switch in endogenous hippocampal microglia and a role in proliferation. J Neurosci 1999; 19:10680-93.
40. Pahapill PA, Schlichter LC. Modulation of potassium channels in intact human T lymphocytes. J Physiol 1992; 445:407-30.
41. Blaustein MP, Lederer WJ. Sodium/calcium exchange: Its physiological implications. Physiol Rev 1999; 79:763-854.
42. Schilling T, Eder C. A novel physiological mechanism of glycine-induced immunomodulation: Na⁺-coupled amino acid transporter currents in cultured brain macrophages. J Physiol 2004; 559:35-40.
43. Myers VB, Haydon DA. Ion transfer across lipid membranes in the presence of gramicidin A. II. The ion selectivity. Biochim Biophys Acta 1972; 274:313-22.
44. Czyz A, Kiedrowski L. In depolarized and glucose-deprived neurons, Na⁺ influx reverses plasmalemmal K⁺-dependent and K⁺-independent Na⁺/Ca²⁺ exchangers and contributes to NMDA excitotoxicity. J Neurochem 2002; 83:1321-8.
45. Levi AJ, Lee CO, Brooksby P. Properties of the fluorescent sodium indicator "SBFI" in rat and rabbit cardiac myocytes. J Cardiovasc Electrophys 1994; 5:241-57.
46. Urbanczyk J, Chernysh O, Condrescu M, Reeves JP. Sodium-calcium exchange does not require allosteric calcium activation at high cytosolic sodium concentrations. J Physiol 2006; 575:693-705.
47. Rae J, Cooper K, Gates P, Watsky M. Low access resistance perforated patch recordings using amphotericin B. J Neurosci Meth 1991; 37:15-26.
48. Matsuda T, Arakawa N, Takuma K, Kishida Y, Kawasaki Y, Sakaue M, Takahashi K, Takahashi T, Suzuki T, Ota T, Hamano-Takahashi A, Onishi M, Tanaka Y, Kameo K, Baba A. SEA0400, a novel and selective inhibitor of the Na⁺-Ca²⁺ exchanger, attenuates reperfusion injury in the in vitro and in vivo cerebral ischemic models. J Pharmacol Exp Ther 2001; 298:249-56.
49. Iwamoto T. Forefront of Na⁺/Ca²⁺ exchanger studies: Molecular pharmacology of Na⁺/Ca²⁺ exchange inhibitors. J Pharmacol Sci 2004; 96:27-32.
50. Boucsein C, Zacharias R, Farber K, Pavlovic S, Hanisch UK, Kettenmann H. Purinergic receptors on microglial cells: Functional expression in acute brain slices and modulation of microglial activation in vitro. Eur J Neurosci 2003; 17:2267-76.
51. Visentin S, Renzi M, Frank C, Greco A, Levi G. Two different ionotropic receptors are activated by ATP in rat microglia. J Physiol 1999; 519:723-36.
52. Xiang Z, Burnstock G. Expression of P2X receptors on rat microglial cells during early development. Glia 2005; 52:119-26.
53. Farber K, Kettenmann H. Purinergic signaling and microglia. Pflugers Arch 2006; 452:615-21.
54. Jiang X, Newell EW, Schlichter LC. Regulation of a TRPM7-like current in rat brain microglia. J Biol Chem 2003; 278:42867-76.
55. Jiang J, Li M, Yue L. Potentiation of TRPM7 inward currents by protons. J Gen Physiol 2005; 126:137-50.
56. Lopez-Redondo F, Nakajima K, Honda S, Kohsaka S. Glutamate transporter GLT-1 is highly expressed in activated microglia following facial nerve axotomy. Mol Brain Res 2000; 76:429-35.
57. Lenart B, Kintner DB, Shull GE, Sun D. Na-K-Cl cotransporter-mediated intracellular Na⁺ accumulation affects Ca²⁺ signaling in astrocytes in an in vitro ischemic model. J Neurosci 2004; 24:9585-97.

58. Chen H, Sun D. The role of Na-K-Cl co-transporter in cerebral ischemia. Neurol Res 2005; 27:280-6.

59. Stiefel MF, Tomita Y, Marmarou A. Secondary ischemia impairing the restoration of ion homeostasis following traumatic brain injury. J Neurosurg 2005; 103:707-14.

60. Silver IA, Erecinska M. Ion homeostasis in rat brain in vivo: Intra- and extracellular [Ca^{2+}] and [H$^+$] in the hippocampus during recovery from short-term, transient ischemia. J Cereb Blood Flow Metab 1992; 12:759-72.

61. Ruknudin AM, Wei SK, Haigney MC, Lederer WJ, Schulze DH. Phosphorylation and other conundrums of Na/Ca exchanger, NCX1. Ann NY Acad Sci 2007; 1099:103-18.

62. Nagano T, Kawasaki Y, Baba A, Takemura M, Matsuda T. Up-regulation of Na$^+$-Ca^{2+} exchange activity by interferon-gamma in cultured rat microglia. J Neurochem 2004; 90:784-91.

63. Andersen JK. Oxidative stress in neurodegeneration: Cause or consequence? Nat Med 2004; 10:S18-25.

64. Simchowitz L. Chemotactic factor-induced activation of Na$^+$/H$^+$ exchange in human neutrophils. II. Intracellular pH changes. J Biol Chem 1985; 260:13248-13255.

65. Schrenzel J, Serrander L, Banfi B, Nusse O, Fouyouzi R, Lew DP, Demaurex N, Krause KH. Electron currents generated by the human phagocyte NADPH oxidase. Nature 1998; 392:734-7.

66. Decoursey TE, Morgan D, Cherny VV. The voltage dependence of NADPH oxidase reveals why phagocytes need proton channels. Nature 2003; 422:531-4.

67. Grinstein S, Foskett JK. Ionic mechanisms of cell volume regulation in leukocytes. Ann Rev Physiol 1990; 52:399-414.

68. Khanna R, Roy L, Zhu X, Schlichter LC. K$^+$ channels and the microglial respiratory burst. Am J Physiol 2001; 280:C796-806.

69. Schlichter LC, Sakellaropoulos G, Ballyk B, Pennefather PS, Phipps DJ. Properties of K$^+$ and Cl$^-$ channels and their involvement in proliferation of rat microglial cells. Glia 1996; 17:225-36.